Effect of Extrusion and Heat Treatment on Microstructure and Mechanical Properties of Mg-1.27Zn-0.75Gd-0.17Zr Alloy

Siqi Yin, Yifan Zhang, Dongting Hou, Guangzong Zhang, and Zhiqiang Zhang

Abstract

Mg-1.27Zn-0.75Gd-0.17Zr alloy (at.%) reinforced by long period stacking ordered (LPSO) structure X-$Mg_{12}GdZn$ was fabricated and then subjected to indirect extrusion and T5 and T6 heat treatments, respectively. Effect of indirect extrusion and heat treatments on microstructure evolution and room temperature tensile mechanical properties were systematically studied and discussed. Results show that the morphology of *X*-phase changes from plate-like to lamellar-like and further to disconnected block-like with the technical process. Large amounts of fine β' phases precipitate in α-Mg matrix of T5-treated alloy. Tensile and yield strength of the as-extruded alloy is 338 and 230 MPa, which is owing to the hard and fragile lamellar-like *X*-phase is easy to start cracks. T5-state alloy exhibits optimal mechanical properties with ultimate tensile strength of 390 MPa, tensile yield strength of 295 MPa and elongation of 11.9%, owing to the β' precipitates strengthening and LPSO *X*-phase strengthening.

S. Yin · Y. Zhang · D. Hou
School of Mechanical Engineering, Dalian Jiaotong University, Dalian, 116028, China
e-mail: yinsiqi89@163.com

Y. Zhang
e-mail: 1940300452@qq.com

D. Hou
e-mail: 21940300452@qq.com

G. Zhang (✉)
Engineering Research Center of Continuous Extrusion, Ministry of Education, Dalian Jiaotong University, Dalian, 116028, China
e-mail: gzzhang@djtu.edu.cn

Z. Zhang
Key Lab of Electromagnetic Processing of Materials, Ministry of Education, Northeastern University, Shenyang, 110819, China
e-mail: zqzhang@mail.neu.edu.cn

Keywords

Mg-Zn-Gd-Zr alloy • Ternary phases • Heat treatment • β' precipitate • Mechanical properties

Introduction

Recently, magnesium alloys have shown the potential to serve as excellent structural and engineering materials that can reduce the weight of vehicle or aerospace components with superior high specific strength and specific stiffness [1, 2]. However, a serious difficulty in further application of magnesium alloys is the poor mechanical properties, especially its low strength and mechanical processing [3].

The strengthening of Mg-based alloys has long been a popular subject for the weight reduction. Mg-Zn-RE alloys have attracted more attention because of the superior mechanical properties. The addition of Zn in Mg-RE alloys has been identified to have significant effect in improving both the strength and ductility [4]. The solid solubility of rare earth element Gd in magnesium alloys reduces dramatically with decreasing temperature, whose equilibrium solid solubility at 821 K and 473 K is 4.53 at.% and 0.61 at.%, respectively, forming an ideal system for precipitation hardening. Thus, magnesium alloys with Gd addition have been extensively studied to develop high strength and good heat-resistance. Anyanwu et al. researched that the as-extruded Mg-17Gd-0.51Zr alloy reaches the ultimate tensile strength of 400 MPa after T5 heat treatment, which was mainly due to the fine precipitates in the matrix during aging [5]. Mg-Zn-Gd alloys with excellent mechanical properties are attributed to solution strengthening, aging strengthening and secondary phases strengthening, especially long period stacking ordered (LPSO) structure X-$Mg_{12}GdZn$ strengthening [6]. Lu et al. [7] investigated that 16 ECAP passed $Mg_{97.1}Zn_1Gd_{1.8}Zr_{0.1}$ (at.%) alloy owns the ultimate tensile strength, yield strength and elongation of

S. Barela et al. (eds.), *Magnesium Technology 2023*, The Minerals, Metals & Materials Series,
https://doi.org/10.1007/978-3-031-22645-8_36

387 MPa, 324 MPa and 23.2%, respectively, which could be attributed to a large number of 14H LPSO *X*-phase.

As a kind of effective strengthening phase, Mg-Zn-Gd alloys with LPSO phase show good possibility to be a type of high-strength magnesium alloys. The accumulated experimental results indicate that the mechanical properties of Mg-Zn-Gd alloys could be tailored by reasonable control of the volume fraction and morphology of the LPSO structures. Simultaneously, Zn and Gd ratio could influence the volume fraction of LPSO *X*-phase and show a range of mechanical properties. More recently, it is believed that the LPSO-containing magnesium alloys demonstrate ordinary performance in as-cast condition, but the mechanical properties are significantly enhanced after conventional plastic deformations such as hot extrusion, equal channel angular pressing (ECAP) process and rolling [8]. Hot extrusion is an extremely effective method to refine the microstructure and phase morphology so as to improve the mechanical properties of magnesium alloys. On the basis of considering technical conditions could also cause the transformation of secondary phase volume fraction and morphology, and the effect and strengthening mechanism have not yet been widely reported.

Based on this background, microstructures and mechanical properties of a Mg-1.27Zn-0.75Gd-0.17Zr alloy during extrusion, and following solution treatment and isothermal aging (T5 and T6 treatments) were investigated in this study, in order to explore the possibility of preparing Mg-Zn-Gd-Zr alloys strengthened via co-existed LPSO phases and precipitates. A trace amount of Zr added into the investigated alloys was aiming at grain refinement.

Materials and Methods

A Φ60 mm Mg-1.27Zn-0.75Gd-0.17Zr (at.%) billet was successfully prepared by conventional casting method [9]. Chemical composition of the alloy is presented in Table 1. Samples cut from the ingot are homogenized at 430 °C for 14 h and quenched into cold water. Indirect extrusion is from Φ47 mm cylinders to Φ12 mm rods with a speed of 5.6 cm s^{-1} in a Φ50 mm extruding container at 400 °C. Aging hardening behaviors are investigated at 200 °C for different times between 2 and 117 h. Parts of the extruded rods and tensile specimens are solution-treated at 430 °C for 8 h, among which a fraction of them is followed by aging at 200 °C to achieve T6-state. T5 processing is performed by aging of the extruded samples directly at 200 °C. Finally, the annealed samples are dipped into the water for quenching.

Tensile tests of the specimens are performed in triplicate at a crosshead speed of 1 mm/min, according to the relevant standard of using cylindrical specimen with the dimension of 25 mm gauge length and 6 mm diameter. All tensile tests are carried out on a Shimadzu AG-X (10 kN) machine at room temperature. Image analysis technique using at least ten areas is applied to estimate the volume fraction of second phase. Vickers hardness test is carried out by 3 kg load for 15 s. Linear intercept method is used to determine the grain size of the alloys. Microstructures are observed by an optical microscope (OM), a transmission electron microscope (TEM; JEM-ARM200F) and a scanning electron microscope (SEM; Zeiss Ultra 55, Germany) with an energy dispersive spectroscope analyzer (EDS). The acceleration voltage of TEM is 200 kV, the corresponding bright-field and high-resolution images are characterized. Similarly, the secondary electron images of SEM are detected, 500–5000 magnifications are used, and the acceleration voltage is 15 kV. Results of diffraction peaks are manipulated through the normalized process.

Results and Discussion

Age hardening behaviors: The age-hardening values with different aging time of the sample aged at 200 °C is shown in Fig. 1. Originally, the hardness value increases slowly and then increases rapidly after 8 h aging. It reaches the peak at 16 h and then decreases gradually. Subsequently, the hardness adopts a saw-tooth-like model with the prolonged aging time and then turns into a period of fluctuation. In order to correlate the hardness with the microstructures, peak hardness of 16 h will be investigated further.

Microstructure evolution: Fig. 2 shows the XRD patterns of the Mg-1.27Zn-0.75Gd-0.17Zr alloy at different conditions. It reveals that as-cast Mg-1.27Zn-0.75Gd-0.17Zr alloy is composed of α-Mg solid solution, *W*-phase ($Mg_3Zn_3Gd_2$), and *X*-phase ($Mg_{12}GdZn$). After the indirect extrusion and the subsequent heat treatments, second phases composition remain the same but diffraction peaks intensity of *X*-phase is stronger than that in as-cast condition, and diffraction peaks intensity of *W*-phase is weaker than the as-cast alloy.

Figure 3 manifests the microstructures of the longitudinal section for the Mg-1.27Zn-0.75Gd-0.17Zr alloy. After

Table 1 Chemical analysis constitution of the experimental alloy

Alloy	Chemical analysis constitution (at. %)			
	Zn	Gd	Zr	Mg
Mg-1.27Zn-0.75Gd-0.17Zr	1.268	0.753	0.171	Bal

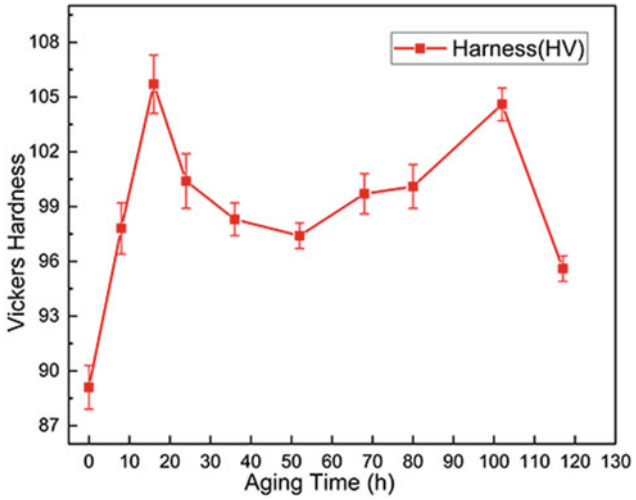

Fig. 1 Age hardening values of experimental alloy

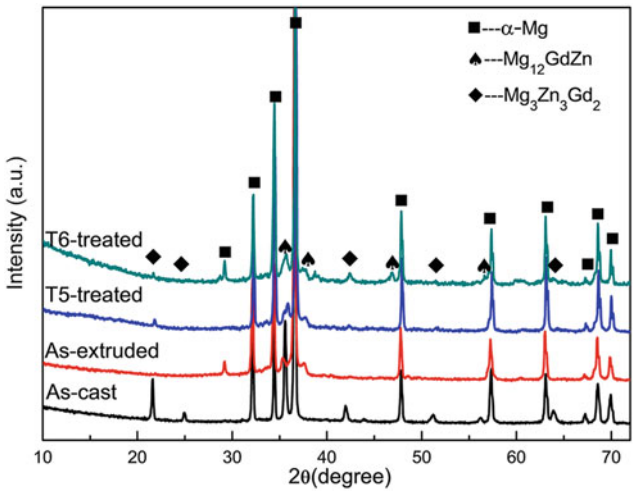

Fig. 2 XRD patterns of the Mg-1.27Zn-0.75Gd-0.17Zr alloy

extrusion and heat treatments, the second phases are cracked and zonal distributing along the extruding direction. Meanwhile, dynamic recrystallization (DRX) occurs during the extrusion process and large amount of dynamic recrystallized (DRXed) grains appear. Average size of the dynamic recrystallization grains ranges from 8 ~ 12 to 10 ~ 15 μm via T5-treated procedure, and it reaches about 18 μm after T6 treatment. This phenomenon illustrates that heat treatment process could coarsen the grains. EDS result of point A suggests that the chemical composition of the block-like phase is Mg-9.17 at. % Zn-6.49 at. % Gd, suggesting it is W-$Mg_3Zn_3Gd_2$ phase. The lamellar-like structure of point B in Fig. 2a contains Mg (88.47 at. %), Zn (5.13 at. %) and Gd (6.36 at. %), which is close to X-$Mg_{12}GdZn$ phase. Volume fraction of the second phases in matrix increase with the process of T5 and T6 treatments. Meanwhile, *X*-phase morphology develops into bulk of thick plates throughout the matrix (Fig. 3e).

The TEM observation and corresponding SAED patterns for the as-annealed specimens are shown in Fig. 4. The 14-layer period-stacking structure *X*-phase is always existed in as-extruded and as-annealed conditions as shown in Fig. 4b and c. Figure 4a shows the TEM bright-field image of the alloy aged at 200 °C for 16 h. A high density of fine spherical precipitates with black contrast could be observed in the grains. These particles are distributing in the matrix uniformly and compactly. According to the corresponding selected area electron diffraction (SAED) pattern given in Fig. 4d, extra diffraction spots of the precipitates are observed at the 1/2 {1–210} and 1/2 {−1012} positions, indicating these precipitates are *β′* phases [10]. Figure 4b shows the image of the alloy at T6 condition. A little bit of small *β′*ellipsoidal particles emerges in the matrix.

The mechanical properties of the alloy in as-extruded condition, T5-state and T6-state are demonstrated in Fig. 5.

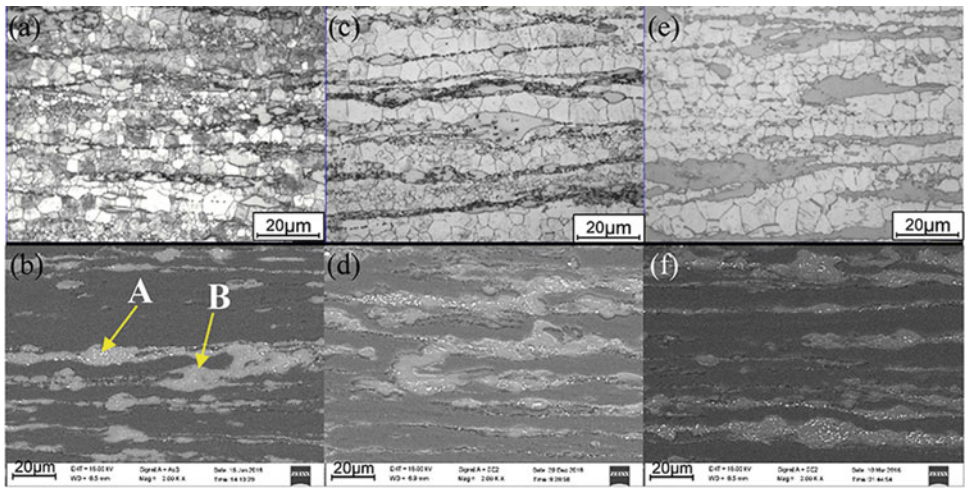

Fig. 3 Microstructures of the Mg-1.27Zn-0.75Gd-0.17Zr alloy: **a** Optical microstructure and **b** SEM image of the as-extruded alloy; **c** Optical microstructure and **d** SEM image of the T5-treated alloy; **e** Optical microstructure and **f** SEM image of the T6-treated alloy

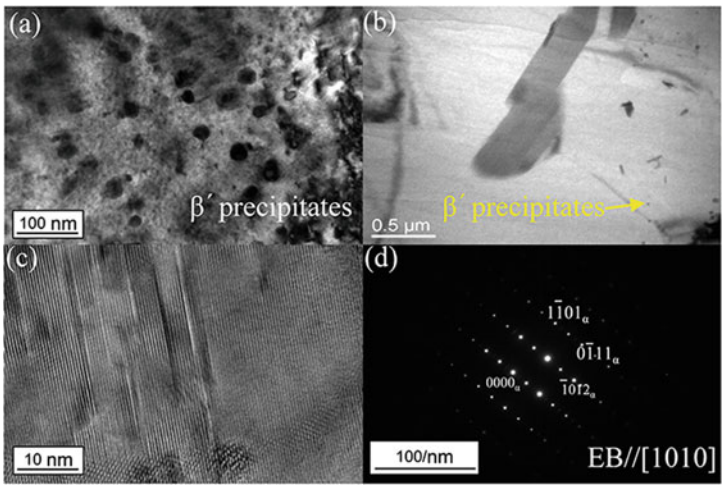

Fig. 4 TEM images and corresponding SAED patterns of the as-annealed experimental alloy: **a** T5-state and **b** T6-state Mg-1.27Zn-0.75Gd-0.17Zr alloy; **c** HRTEM image of T6-state Mg-1.27Zn-0.75Gd-0.17Zr alloy and **d** corresponding SAED pattern of (**a**)

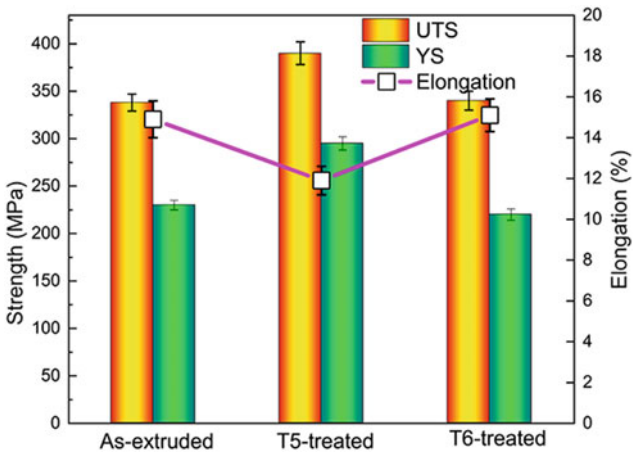

Fig. 5 Tensile properties of the experimental alloy at different conditions

With the peak-aging treatment at 200 °C for 16 h, the ultimate tensile strength is improved from 338 to 390 MPa. However, the elongation of the alloy is decreased from 14.9 to 11.9%. Nevertheless, ultimate tensile strength decreases to 340 MPa and the elongation slightly increases to 15.1% after the solution and aging treatment (T6). Generally speaking, volume fraction of second phases increases gradually than the extruded condition. Meanwhile, *X*-phase morphology develops into bulk of thick plates throughout the matrix (Fig. 3e). Although the aging treatment at 200 °C does not affect the volume fraction of LPSO *X*-phase in the alloy, it has a significant effect on the formation of RE precipitates. With prolonged aging at 200 °C, large amount of RE precipitates (*β′* phases) is formed in α-Mg matrix of the alloy and its volume fraction also increased gradually. The large amount of fine, dense and uniformly dispersed β′ phases precipitate in the T5-treated alloy contribute to the high strength and good thermal stability of the alloy. The precipitates have great ability to retard dislocation motion on the basal planes [11]. The *β′* precipitates form on the prismatic planes and the LPSO structures form on the basal planes, interconnecting into a network within the alloy and thus leading to the unique mechanical properties of the alloy.

To sum up, aging (T5) treatment is the effective measure to strengthen the LPSO *X*-phase containing alloys. The worse mechanical properties of T6-staged alloy may be attributed to the dissevered effect of plate-shaped *X*-phase and the relatively large DRXed grains. In the meanwhile, strengthening precipitate can easily change the semi-coherent crystal lattice with high solid solution temperature, so as to decrease the strengthening effect.

Conclusion

1. Mg-1.27Zn-0.75Gd-0.17Zr (at.%) alloy consists of α-Mg, *X*-phase and *W*-phase. Volume fraction of secondary phases increase through heat treatments, but the second phase species remain unchanged.

2. Large amounts of fine β′ phases precipitate in α-Mg matrix of T5-treated alloy. The alloy owns the superior ultimate and yield strength of 390 and 295 MPa at T5-state, respectively, as well as the elongation of 11.9%.

3. Little *β′*ellipsoidal particles emerge in the matrix after T6 treatment. Through T6 treatment, the ultimate and yield strength is 340 and 220 MPa, the elongation is 15.1%.

Acknowledgements This research was financially supported by "Double Tops" Construction Program of Liaoning Province [grant nos. 032077 and 032089] and National Natural Science Foundation of Liaoning Province [grant nos. 2022-BS-261 and 2022-BS-262].

References

1. Joost WJ, Krajewski PE (2017) Towards magnesium alloys for high-volume automotive applications. Scr. Mater. 128:107-112.
2. Yamasaki M, Hashimoto K, Hagihara K, Kawamura Y (2011) Effect of multimodal microstructure evolution on mechanical properties of Mg-Zn-Y extruded alloy. Acta. Mater. 59:3646-3658.
3. Hagihara K, Kinoshita A, Sugino Y, Yamasaki M, Kawamura Y, Yasuda HY, Umakoshi Y (2010) Ultra high-strength Mg-Gd-Y-Zn-Zr alloy sheets processed by large-strain hot rolling and ageing. Acta. Mater. 58:6282-6293.
4. Matsuda M, Ii S, Kawamura Y, Ikuhara Y, Nishida M (2004) Enhanced age hardening response and creep resistance of Mg-Gd alloys containing Zn. Mater. Sci. Eng. A. 386:447-452.
5. Anyanwu IA, Kamado S, Kojima Y (2011) Creep properties of Mg-Gd-Y-Zr alloys. Mater. Trans. 42:1212-1218.
6. Zhang XB, Wang Q, Chen F, Wu YJ, Wang ZZ, Wang Q (2015) Relation between LPSO structure and biocorrosion behavior of biodegradable GZ51K alloy. Mater. Lett. 138:132-135.
7. Lu F, Ma A, Jiang J, Yang D, Song D, Yuan Y, Chen J (2014) Effect of multi-pass equal channel angula rpressing on microstructure and mechanical properties of $Mg_{97.1}Zn_1Gd_{1.8}Zr_{0.1}$ alloy. Mater. Sci. Eng. A. 594:330-333.
8. Wang JF, Song PF, Gao S, Huang XF, Shi ZZ, Pan FS (2011) Effects of Zn on the microstructure, mechanical properties, and damping capacity of Mg-Zn-Y-Zr alloys. Mate. Sci. Eng. A. 528:5914-5920.
9. Yin SQ, Duan WC, Liu WH, Wu L, Yu J M, Zhao ZL, Liu M, Wang P, Cui JZ, Zhang ZQ (2020) Influence of specific second phases on corrosion behaviors of Mg-Zn-Gd-Zr alloys. Corros. Sci. 166:108419.
10. Liu XB, Chen RS, Han EH (2008) Effects of ageing treatment on microstructures and properties of Mg-Gd-Y-Zr alloys with and without Zn additions. J. Alloys Compd. 465:232-238.
11. Nie JF (2003) Effects of precipitate shape and orientation on dispersion strengthening in magnesium alloys. Scr. Mater. 48:1009-1015.